Video Article

Nanomanipulation of Single RNA Molecules by Optical Tweezers

William Stephenson[1], Gorby Wan[2], Scott A. Tenenbaum[3,4], Pan T. X. Li[4,5]

[1]Nanoscale Engineering Graduate Program, College of Nanoscale Science and Engineering, University at Albany, State University of New York

[2]Nanoscale Science Undergraduate Program, College of Nanoscale Science and Engineering, University at Albany, State University of New York

[3]Nanobioscience Constellation, College of Nanoscale Science and Engineering, University at Albany, State University of New York

[4]The RNA Institute, University at Albany, State University of New York

[5]Department of Biological Sciences, University at Albany, State University of New York

Correspondence to: Pan T. X. Li at pli@albany.edu

URL: https://www.jove.com/video/51542
DOI: doi:10.3791/51542

Keywords: Bioengineering, Issue 90, RNA folding, single-molecule, optical tweezers, nanomanipulation, RNA secondary structure, RNA tertiary structure

Date Published: 8/20/2014

Citation: Stephenson, W., Wan, G., Tenenbaum, S.A., Li, P.T. Nanomanipulation of Single RNA Molecules by Optical Tweezers. *J. Vis. Exp.* (90), e51542, doi:10.3791/51542 (2014).

Abstract

A large portion of the human genome is transcribed but not translated. In this post genomic era, regulatory functions of RNA have been shown to be increasingly important. As RNA function often depends on its ability to adopt alternative structures, it is difficult to predict RNA three-dimensional structures directly from sequence. Single-molecule approaches show potentials to solve the problem of RNA structural polymorphism by monitoring molecular structures one molecule at a time. This work presents a method to precisely manipulate the folding and structure of single RNA molecules using optical tweezers. First, methods to synthesize molecules suitable for single-molecule mechanical work are described. Next, various calibration procedures to ensure the proper operations of the optical tweezers are discussed. Next, various experiments are explained. To demonstrate the utility of the technique, results of mechanically unfolding RNA hairpins and a single RNA kissing complex are used as evidence. In these examples, the nanomanipulation technique was used to study folding of each structural domain, including secondary and tertiary, independently. Lastly, the limitations and future applications of the method are discussed.

Video Link

The video component of this article can be found at https://www.jove.com/video/51542/

Introduction

The development of the optical tweezers technique has long been accompanied with its application in biological research. When the optical trapping effect was first discovered, Arthur Ashkin observed that bacteria in contaminated water could be trapped at the laser focus[1]. Since then, bacteria trapping has become an unintentional, fun experiment for generations of biophysics students as well as a serious research tool to study microbial physiology[2,3]. The optical trapping technique uses focused laser beam to immobilize a microscopic object[1]. Practically, a laser trap functions as an optical spring, which also measures force (F) on the trapped object by its displacement from the center of the trap (ΔX). Within a short range, $F = \kappa x \Delta X$, in κ is the spring constant of the trap. The optical trap can be used to exert force in picoNewton (pN) precision to a microscopic object and measure its position with nanometer (nm) accuracy. In the past two decades, optical tweezers have become one of the most used single-molecule techniques in biophysics. The technique has been employed to study folding and mechanics of DNA[4-6], RNA[7-9], and proteins[10,11]. Optical tweezers have also been used to observe DNA replication[12], RNA transcription[13], and protein synthesis[14,15], as well as many other biomolecular events[16-18].

Single-molecule approaches are employed in RNA structural research mainly to explore the rugged folding energy landscape of RNA. An RNA sequence can usually fold into multiple stable, mutually exclusive structures, due to the simple chemical composition and base paring rules of RNA. It has long been known that RNA structural polymorphism, such as that occurs in riboswitches[19,20], plays an important role in gene regulation. A recent genome-wide survey has revealed that temperature variations as small as a few degrees greatly influence structure and protein synthesis of a large portion of the cellular transcriptome[21]. This example hints that the biological role of alternative RNA folding is perhaps more important and pervasive than previously assumed. Structural polymorphism, however, poses a challenge for the traditional biochemical and biophysical approaches, which examine average properties of many molecules. For example, the “on” and “off” conformations of a riboswitch are mutually exclusive. An averaged structure derived from heterogeneous structures is not likely to resemble either of the biologically relevant conformers. Moreover, untranslated RNA and mRNA usually form structures. Their interaction with proteins and regulatory RNAs commonly requires unfolding of existing structure as part of the interaction. Therefore, studying RNA unfolding/refolding becomes a pertinent issue of RNA biology. To meet such a challenge, the single-molecule approach has been employed to unravel RNA structural polymorphism by studying one molecule at a time[22-27].

As compared to the popular single-molecule fluorescence method, tweezers based mechanical unfolding offers an advantage that conformations of individual molecules can be manipulated by applied force and be measured with nanometer precision. This nanomanipulation capability can

Copyright © 2014 Journal of Visualized Experiments

be utilized to monitor the unfolding/folding of individual structural domains such that the hierarchical folding of a large RNA can be dissected[28]. Alternatively, a single strand can be directed to fold into one of several conformers; or an existing structure can be mechanically induced to refold into a different conformation[29]. Under biological conditions, an RNA structure can be altered upon temperature change or ligand binding. The capability of directly manipulating molecular structure opens a new venue of RNA structural study. In principle, other mechanical techniques, such as atomic force microscope and magnetic tweezers, can also be used to study folding of single RNA molecules. However, such applications are limited largely due to the relatively low spatial resolution[30].

The employment of optical tweezers allows RNA structures to be unfolded by mechanical force.

The advantage of mechanical unfolding is several fold. Force can be used to unfold both secondary and tertiary structures, whereas metal ions and ligand induced folding are mainly limited to tertiary structures. Temperature and denaturant can significantly affect the activities of water and solutes. In contrast, force is applied locally to perturb molecular structures; the effect of force on the surrounding environment is negligible. In addition, thermal melting is best used to study folding thermodynamics of small RNA structures, whereas optical tweezers have been used to study RNA structures with various sizes, ranging from a seven-base-pair tetraloop hairpin[28] to a 400-nucleotide ribozyme[31]. Furthermore, RNA structures can be mechanically unfolded at mesophilic temperatures. In contrast, to unfold RNAs in a thermal melting experiment, temperature is typically raised well above physiological temperatures, which significantly increases RNA hydrolysis, especially in the presence of Mg^{2+} ions.

It is important to note that the mechanical effect of force depends on how it is applied to a structure. The applied force tilts the folding energy landscape. For example, when force is applied to a hairpin, the base pairs are sequentially broken, one at a time (**Figure 1a**). The ripping fork progresses along the helical axis, which is perpendicular to the applied force. In contrast, when a minimal kissing complex is under tension, the two kissing base pairs, which are parallel to the applied force, share the force load (**Figure 1b**). The different geometries of the hairpin and kissing complex relative to the applied force result in their different mechanical response, which can be utilized to distinguish secondary and tertiary folding[28,32]. The theoretic aspect of mechanical unfolding has been previously reviewed[8,9,30]. This work outlines the basic approaches to set up and perform a single-molecule mechanical unfolding assay.

Experimental Setup. In our mechanical pulling experiment, the RNA sample for tweezing consists of the RNA of interest flanked by two double-stranded DNA/RNA handles (**Figure 2**)[7]. The entire molecule can be tethered to two surface-coated micron-size beads (Spherotech) via streptavidin-biotin and digoxigenin-anti-digoxigenin antibody interactions, respectively. One bead is held by a force-measuring optical trap, whereas the other is held on the tip of a micropipette. The relative distance between the beads can be changed by either steering the trap or moving the micropipette. Using this approach, a single RNA molecule tethering the beads can be stretched and relaxed.

Preparation of Samples. The synthesis of RNA samples for tweezing includes a few steps (**Figure 3**). First, the DNA sequence corresponding to the RNA of interest is first cloned into a plasmid vector. Next, three PCR reactions are performed to generate the two handles and a template for transcription. The transcription template encompasses the handle regions and the inserted sequences. The full length RNA is synthesized by *in vitro* transcription. Last, the RNA and chemically modified handles are annealed together to generate the molecules for tweezing.

Calibration and Operation of Tweezers. The basic design of the Minitweezers used in this work follows that of the dual-beam optical tweezers[33]. With many improvements, the Minitweezers display extraordinary stability as compared to the first generation optical tweezers. A number of research groups in several countries use the Minitweezers in their single-molecule research[14,15,34-37]. The details of construction, calibration, and operation of the device, including instruction videos, are available at the “Tweezers Lab” website (http://tweezerslab.unipr.it). Here, improvements and calibration procedures that need to be performed on daily bases are described in detail.

Protocol

1. Preparation of RNA Molecules for Single-molecule Tweezing

1. Cloning the sequence of interest. Clone the DNA sequence corresponding to the RNA structure into a vector.
2. Synthesis and purification of the transcription template. Synthesize a transcription template by PCR. [place table 1 here] Next, purify the PCR products using a PCR purification kit, and concentrate the sample to >200 ng/µl. Because the purified DNA is used for transcription, RNase free water should be used in the elution and concentration steps.
3. *In vitro* transcription. Synthesize RNA by *in vitro* transcription at 37 °C overnight to maximize RNA yield. [place table 2 here] After transcription, add 1 µl DNase I to digest the DNA template for 15 min at 37 °C. Purify the RNA using a silica spin column.
4. Synthesis of the biotinylated handle A. First, produce the unmodified handle A by PCR using primers Af and Ar and concentrate the amplified DNA to >200 ng/µl. Next, incorporate biotin modifications into the PCR product using a primer extension reaction. [place table 3 here] NOTE: The biotinylated handle A (biotin-HA) can be directly used in the annealing without purification. As the biotin-HA is to be annealed with RNA, it is critical to use RNase free water in both steps.
5. Synthesis of the digoxigenin-modified handle B. Synthesize digoxigenin modified handle B (dig-HB) by PCR using primer Bf and digoxigenin-modified oligo Dig-Br (**Figure 3**). Next, purify the PCR product and concentrate the sample to >200 ng/µl.
6. Annealing RNA to the handles. Anneal the RNA with handles. [place tables 4 and 5 here]
7. Purify annealed sample. Add 3 volumes of ethanol of the annealed sample and mix well. Store the mixture at -70 °C for at least 1 hr. Spin down at 15,800 x g and discard supernatant. Dry the pellet using a lyophilizer. Dissolve the pellet in 100 µl RNase free water. NOTE: The sample is ready to be used and can be stored at -20 °C.

2. Calibration and Operation of the Optical Tweezers

1. Calibrate Pixel Size of Video Monitor
    1. Use the optical trap to trap a bead with known diameter (size standard).
    2. Capture images of a trapped bead using imaging software (**Figure 4**).

3. Determine the diameter of the bead using the imaging software based on the centroid method.
4. Repeat this procedure to determine diameters of beads of different size.
5. Fit the measured and known diameters of the beads by a linear regression to obtain the physical size of a pixel.

2. Verify Distance Calibration
   1. Use the optical trap to trap a bead.
   2. Determine the pixel position of its centroid by the image capture software and record its position using the Minitweezers.
   3. Steer the bead to different positions and repeat the position determination.
   4. Convert the X and Y positions of the bead from pixels to m unit using the calibrated pixel size.
   5. Compare the X and Y between positions measured by video and by the Minitweezers. The two sets of values should agree. As the image resolution is > 0.1 μm, move the bead over 1 μm between measurements to ensure accuracy. If the distance calibration is not comparable to the one stored in the Minitweezers, recalibrate the instrument.

3. Trap Stiffness Calibration
   1. Capture a bead using the optical trap and hold it still.
   2. Record the force of the trap using a bypass fast data acquisition at a rate > 5 kHz for 3 sec.
   3. Generate a power spectrum from the recording of the bead motion using software. Fit the power spectrum to a Lorentzian (**Figure 5**)[38]:

$$S(f) = {S_0 f_c^2}/{(f_c^2 + f^2)} \quad \text{(Eq. 1)}$$

   in which *S(f)* is the power at the frequency of *f*, f_c is the corner frequency, and S_0 is the asymptotic power. The corner frequency, f_c, is the frequency where the power of thermal motion has decreased to half of the asymptotic value. As f_c varies with laser power and bead size, calibrate each trapped bead individually.
   4. Compute the spring constant of the trap, κ, from f_c:

$$\kappa = 2\pi\gamma f_c \quad \text{(Eq. 2)}$$

   in which γ is the drag coefficient of the bead (Eq. 3). Use the spring constant to determine extension changes of an RNA from force change.

4. Stokes' Law Test
   1. Capture a bead using the optical trap. Move the bead back-and-force at different speed.
   2. Record the motion of the bead and force using the Minitweezers.
   3. Compute the radius of the bead.
   NOTE: The frictional force, F_d, generated by the motion of a spherical particle in a fluid can be described by the Stokes' law:

$$F_d = \gamma v = 6\pi\eta r v \quad \text{(Eq. 3)}$$

   in which *r* is the radius of the sphere, *v* is the velocity, and *h* is the dynamic viscosity of the fluid, which can be found in reference tables. Using the measured force as F_d, the radius of the bead can be computed using Eq. 3 (**Figure 6**) and should agree with that determined by the image acquisition software. The Stokes' law test effectively tests the overall calibrations and performance of the instrument.

3. Nanomanipulation of Single RNA Molecules

1. Making fluidics.
   1. Drill six holes (2 mm diameter each) on a No. 2 cover glass (**Figure 7a**) and cut three slits (2 mm width) into double-sided polyimide tape (**Figure 7b**) using a laser engraver.
   2. Make a flow chamber by sandwiching two cover glass with two layers of double-sided Kapton tape. Insert a micropipette and two bypass tubes between the tape (**Figure 7c**).
   3. Mount the flow chamber onto a metal frame by matching fluidic holes (**Figure 7d**).
   4. Connect the fluidic channels of the chamber to 10 ml syringes filled with buffer of choice via polyethylene tubings (**Figure 7e**).
   5. Mount the entire chamber onto the optical tweezers between the two objectives. Ensure that the front side of the chamber with the fluidic channels faces to the right. Retract the right objective and plug the brass pins of the frame (**Figure 7e**) to mounting holes on the tweezers. Tighten screws to fix the chamber position.

2. Mixing the annealed sample and beads. Mix the annealed sample with anti-digoxigenin-coated beads (dig-beads), and let the mixture to stay at room temperature for 5-10 min. Typically, 1 μl of annealed sample is mixed with 5 μl dig-beads in 1 ml of buffer. NOTE: The amount of the beads to be loaded into the flow chamber should be chosen to ensure a reasonable quantity of the beads to be delivered from the bypassing tube. The ratio of the annealed sample to the beads cannot be easily quantified. In an ideal case, most beads have no RNA such that only a small fraction of beads may have only one RNA molecule per bead. As the annealed samples and the bead suspension are difficult to quantify, the best and only way currently is to vary the mixing ratio and test the mixture on the tweezers.
3. Deliver beads to the reaction site in the flow chamber (*i.e.*, a few micrometers on top of the micropipette tip, **Figure 7c**).
   1. Load a suspension of streptavidin-coated beads (strep-beads) into a 1 ml syringe.
   2. Connect the syringe to the fluidic tubing leading to the bottom channel of the flow chamber (**Figure 7a**).
   3. Push the syringe to flow the strep-beads into the chamber.
   4. Move the entire chamber using motor control software to place the optical trap near the opening of the bottom bypass tube (**Figure 7b**). Then operate the optical trap by a trackball to capture a strep-bead.
   5. Move the bead close to the tip of the micropipette using the motor control software.

6. Pull the syringe connected to the micropipette to suck the bead onto the micropipette.
7. Apply flow gently by pressing the syringe to the middle channel to flush out extra strep-beads.
8. Similarly, deliver the mixture of sample and the dig-beads (see step 3.2) to the top channel of the chamber.
9. Capture a dig-bead and bring it close to the strep-bead using the optical trap.
10. Clean the middle channel by applying flow. NOTE: The strep- and dig-beads are chosen to be different sizes so that they can be distinguished visually under the microscopic view (**Figure 4**).

4. Fishing" a single-molecule tethering between a pair of beads.
    1. Place the dig-bead vertically on top of the strep-bead (**Figure 4**).
    2. Move the dig-bead down towards the strep-bead by steering the trap. Open a force-distance plot window on computer to visualize force changes.
    3. Upon contact of the two beads, move the dig-bead vertically away from the strep-bead.
    4. If no specific contact is made, the force remains almost zero. If the two beads are connected by molecules, the force increases significantly when the two beads separate. This procedure, commonly referred to as "fishing", is often performed multiple times on each pair of beads to find an effective single-molecule tether.

Representative Results

Limited by space, nanomanipulation of single RNA molecules is demonstrated by showing only mechanical unfolding examples of RNA hairpins and an RNA with tertiary structure.

Manipulate Single Hairpin Molecules

Once a tether is established between the beads, extension of and force on the tether can be manipulated using a user-defined protocol. Four common manipulation protocols are commonly used.

Force-ramp Experiment. The most intuitive and common experiment to manipulate a single RNA is to repeatedly stretch and relax the molecule in the direction of the helical axis of the handles (vertically as shown in the **Figure 4**). The force, *F*, and trap position, *Y*, are recorded as a function of time. The extension of the molecule, *e*, can be computed by $e = Y - F/k$, in which is the spring constant of the trap. The pulling result can be displayed as the force-extension curve (**Figure 8a**). The stretching of the double-stranded handles is shown by the rising curve with positive slope. The relaxation curve of the handles retraces that of the stretching. The structural transition of a simple, two-state-folding hairpin displays a "rip" with negative slope, indicating a single, cooperative unfolding transition[39]. The refolding of the hairpin is indicated by a "zip" on the force-extension curve. Importantly, the same molecule may be unfolded and refolded at different forces each time. Such a trend is evident on the distributions of the transition forces (**Figure 8b**). Commonly, the force is changed as a linear function of time, *i.e.*, at a fixed loading/unloading rate. Under a constant loading/unloading rate, the force dependent kinetics can be extracted from distributions of the transition forces[40-42].

Constant Force Experiment. Under the constant force mode, the instrument employs a feedback mechanism to compensate the force deviations from a set value. The extension of an RNA molecule is recorded as a function of time (**Figure 9**)**.** Setting the force at or near the transition force of the particular RNA molecule transition allows for the observation and quantification of molecular extensional states. The lifetimes of the molecule at each state can be pooled together to compute the kinetics of structural transition[7]. The constant force experiment is used to monitor reversible folding, such as those of hairpins[7,28].

Force Jump Experiment. In a force jump experiment, the force is rapidly changed into a different value and kept constant; the lifetime of the first transition is monitored[43]. The force jump is particularly useful to characterize the kinetics of irreversible processes, because the lifetimes of the forward and reverse reactions can be directly measured separately at different forces. At each force jump/drop, only one lifetime is observed. Therefore, multiple rounds of such experiments need to be performed in order to collect sufficient observations to extract kinetics.

Passive Experiments. Under the passive mode, the positions of the trap and the micropipette are both fixed (**Figure 10**). A hairpin exhibits two states corresponding to unfolded and folded RNA near its transition forces. Unlike the constant force experiment, both the force and extension of the molecule change upon the structural transition. Eliminating feedback control allows molecular transitions to be directly monitored without external interference. However, it is difficult to maintain constant force under the passive mode reveals. As the trapped bead diffuse in the optical trap, force changes accordingly. The passive mode is unsuitable for measuring molecular states with long dwell time, during which force is significantly altered. The pros and cons of the constant force and passive modes have been extensively studied and discussed[44].

Unravel Folding of Secondary and Tertiary Structures

Mechanical unfolding of a two-base-pair kissing RNA formed by two linked GACG tetraloop hairpins is used as an example here (**Figure 11a**). Both hairpins an 9-base-pair stem, though the stem sequences are different. The mechanical unfolding path of the RNA (**Figure 11a**) has been characterized by force ramp methods[34]. When force is raised, the kissing complex is first broken, followed by sequential unfolding of the hairpins. On refolding, the hairpins fold first, followed by a kissing interaction at low force. These transitions are visible on the force-extension curve (**Figure 11b**). To confirm the assignment of the hairpin transitions, each of the hairpins can be individually studied. The assignment of the unkissing/kissing transitions can be verified by studying a mutant RNA, in which the tetraloops are mutated to prevent formation of the kissing interaction[28]. Alternatively, the lowest force can be set at 10 pN, higher than the kissing forces. As expected, the force-extension curve under such conditions displays only the unfolding/refolding of the hairpins (**Figure 11c**)[34]. Therefore, it is possible to investigate folding the kissing interaction and each of the two hairpins independently at different forces.

It is noticeable that the folding of the two hairpins is reversible, whereas the kissing interaction is highly irreversible, as evident by very different unkissing and kissing forces, and by large hysteresis. Therefore, the folding kinetics of the hairpins can be studied directly using the constant force experiments. The kinetics of the kissing interaction, however, must be measured using the force jump method. The **Figure 12a** shows a typical force jump experiment[28]. At 3 pN, the entire RNA is folded. The force is then rapidly raised to 22 pN and kept constant. After a few

seconds, the entire RNA is unfolded into a single strand, as evident by a sudden increase of extension of ~30 nm. The force is then raised to 30 pN to further stretch the RNA, before it is lowered to 13 pN. After folding of the hairpins, the force is quickly dropped to 8 pN. The formation of the kissing complex is indicated by shortening of the extension by ~7-8 nm. By collecting many of these lifetime measurements, unkissing and kissing kinetics at constant forces can be computed.

Under all experimental conditions, the kissing complex is always unfolded first. At forces that the hairpins are unstable by themselves, the kissing interaction protects the hairpin structures from unfolding. Such a rate-limiting effect is also revealed by force jump experiments. As shown in the **Figure 12b**[28], when the force is jumped to 16 pN, the extension of the molecule remains largely unchanged for a few seconds, followed by an unfolding increasing the extension by ~20 nm. The changes in the extension indicated the weaker seven-base-pair hairpin is unfolded right after disrupt of the kissing complex. The metastability of the hairpin is evident by the lifetimes. Once the kissing is broken, the hairpin rapidly transits between folded and unfolded states; the lifetimes are less than 1 sec. Essentially, this observation is a constant force experiment for unfolding the hairpin. In contrast, it takes over 10 sec to break the kissing complex along with the hairpin. Similarly, force is jumped to 17.7 pN (**Figure 12c**), at which the entire RNA is unfolded into a single strand, as evident by the increase in the extension of ~30 nm. The bistability of the large, 11-base-pair hairpin can be seen as the extension hops between two values. Again, the short lifetimes of the hairpin are in sharp contrast to its long lifetime in the metastable state. Using a combination of force ramp and force jump experiments, the thermodynamics and kinetics of individual unfolding/folding steps can be measured[28]. Direct observations of the breaking and formation of the kissing complex enables us to analyze energetic contributions of flanking bases to the minimal kissing complex[34] and to measure the salt dependence of the kissing interaction[45].

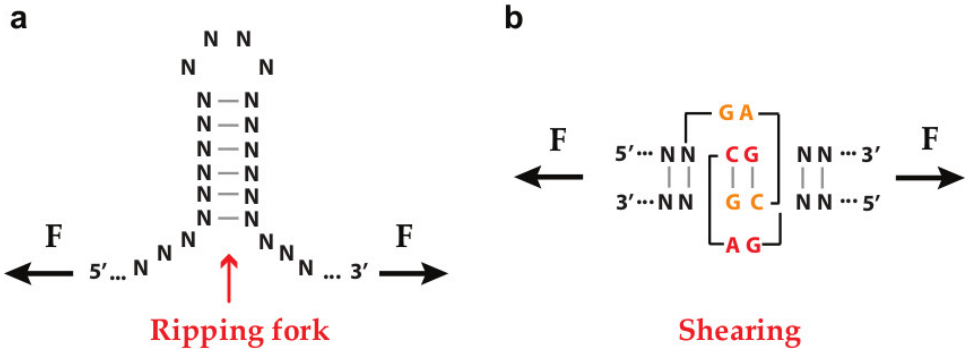

Figure 1. RNA structures relative to the applied force. a) A hairpin under tension. **b)** Pulling a two-base-pair kissing complex. The two hairpin loops are colored in red and yellow.

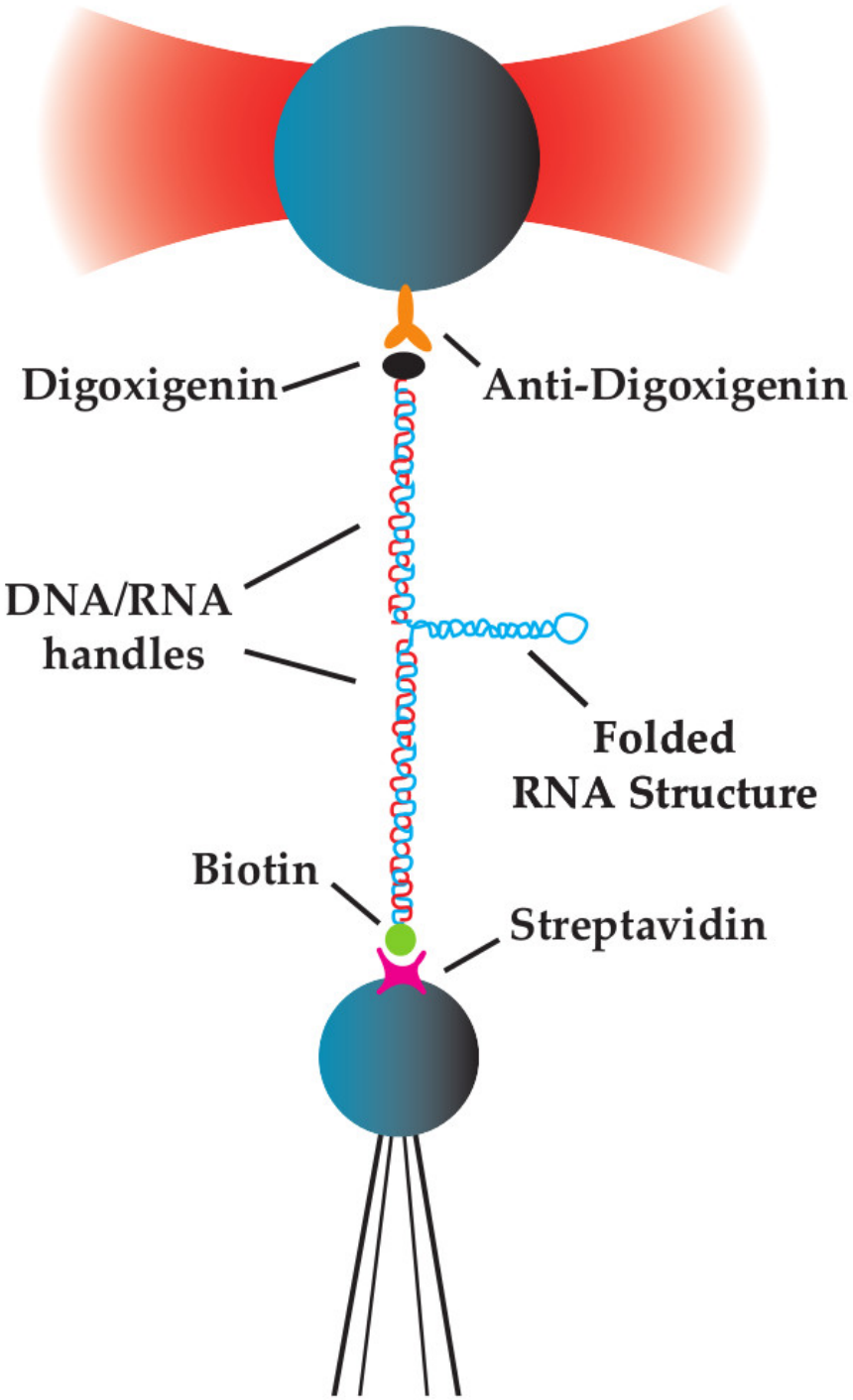

Figure 2. Experimental setup. The RNA structure is flanked by two DNA/RNA handles. Through the chemical modifications on the ends of the handles, the entire molecule can be connected to a pair of protein coated micron-sized beads. One of the beads is held by a steerable, force-measuring optical trap. The other is placed on a micropipette, which is driven by a piezoelectric flexture stage. The drawing is not to scale.

Copyright © 2014 Journal of Visualized Experiments

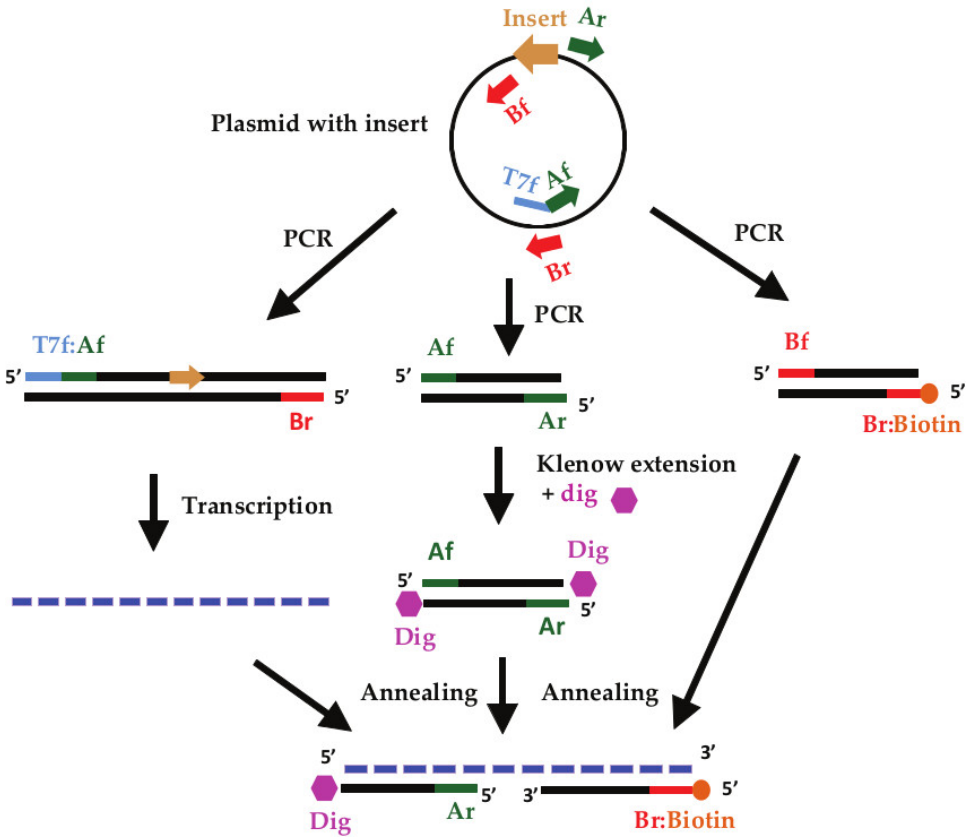

Figure 3. A general scheme to synthesize RNA molecules with handles. The handle A, handle B, and transcription template are generated by PCR from a plasmid with the RNA sequence cloned. The handle A is modified by digoxigenins (dig) at the 3' ends. The handle B has a biotin modification at 5' end of one strand. The full length RNA is transcribed from the transcription template. The RNA and modified handles are mixed and annealed. The properly molecules can be tethered to a pair of beads coated by streptavidin and anti-digoxigenin antibody. The drawing is not to scale.

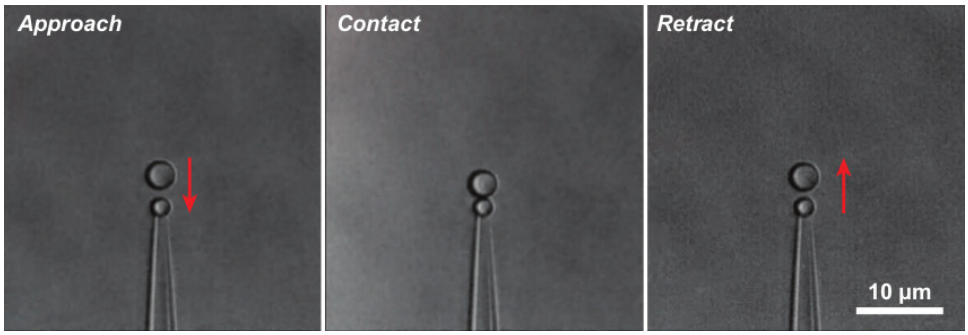

Figure 4. Images of fishing a single-molecule between two beads captured by the video card. One bead is placed on the tip of a micropipette by suction. The other is held and steered by a force-measuring optical trap. The directions of the trap movements are indicated by arrows. The trapped bead first moves vertically towards the bead on the micropipette. Upon contacts, the trapped bead moves up. If a tether is established between the beads, the separation of beads pulls on the molecule and force increases as the molecule is extended. If two beads are not linked by any molecule, the retract motion generates no force.

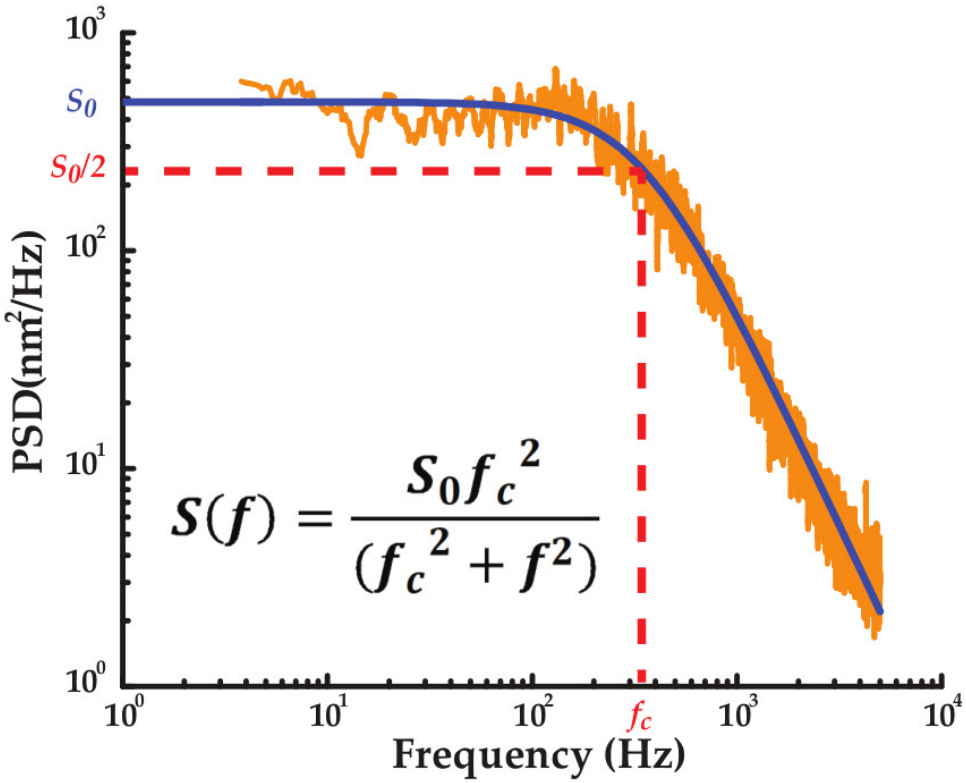

Figure 5. A power spectrum of the Brownian motion of a trapped bead. The solid curve is a fit to the Lorentzian equation (Eq. 1), shown in the insert. The spring constant of the trap can be computed from the corner frequency (Eq. 2).

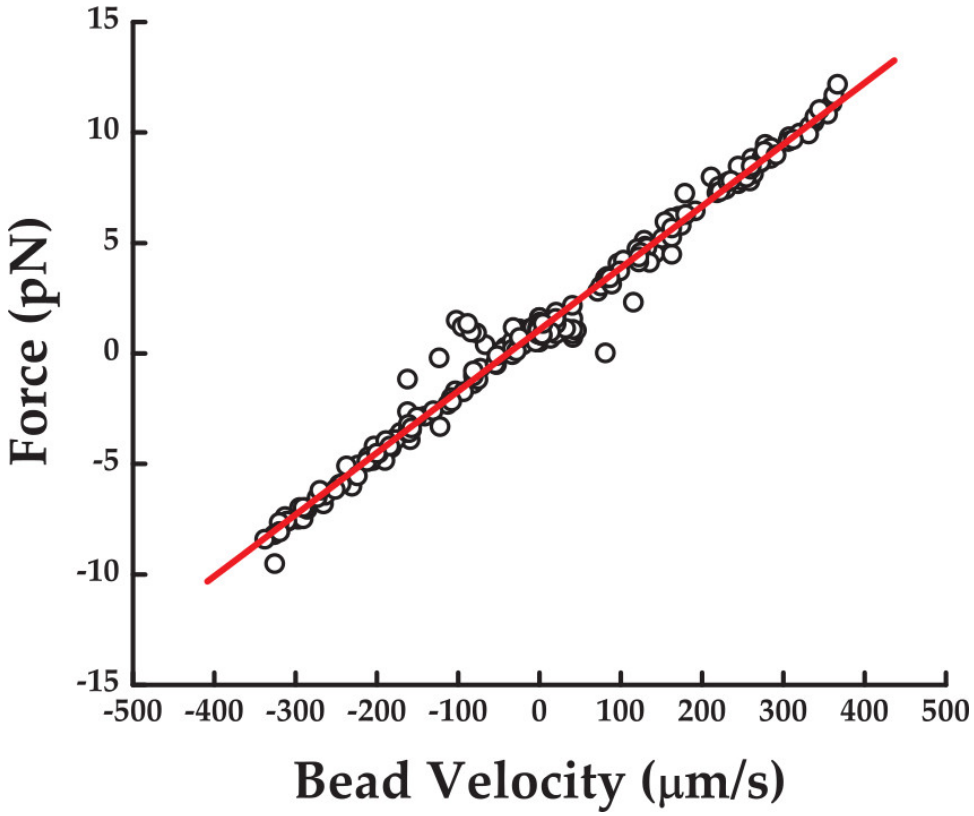

Figure 6. An example of the Stokes' law test. A trapped bead is dragged through water by the oscillating trap. Its velocity and drag force are fit to the Stokes' equation (Eq. 3). From the slope of the fitted line, the bead radius was determined to be 1.66 ± 0.03 μm, which is in good agreement with 1.6 ± 0.2 μm, measured by video images.

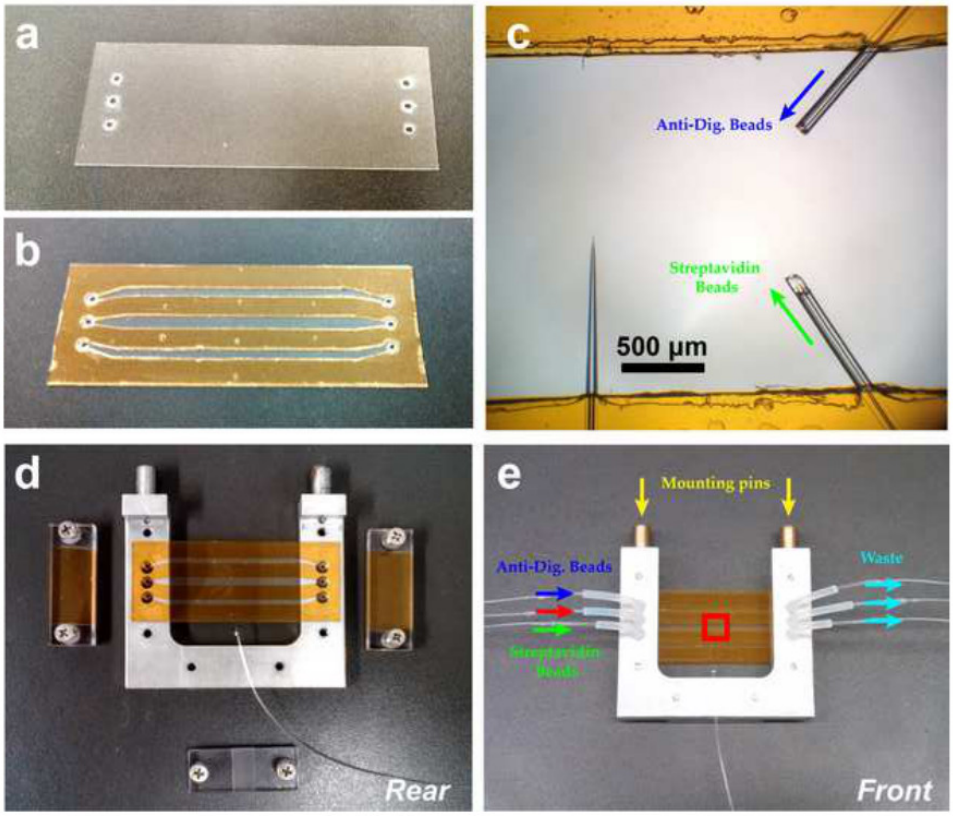

Figure 7. A flow chamber for tweezing. a) Six holes, each with a diameter of 2 mm, are drilled into a No. 2 cover glass by using a laser engraver. **b)** Three 2 mm-wide slits are cut into double-sided polyimide tapes. **c)** A close look at the experimental region containing the micropipette and two bypass tubes. The beads from the top and bottom channels traverse through their respective bypass tubes (blue and green) to the central channel in the directions indicated by arrows. **d)** Mount the fluidic chamber onto a metal frame by matching fluidic holes. **e)** A three-channel chamber connected to flow pipes. The central channel is used for pulling RNA. The top (blue) and bottom (green) channels are used for delivering beads. The experimental region is indicated by a red square.

Copyright © 2014 Journal of Visualized Experiments

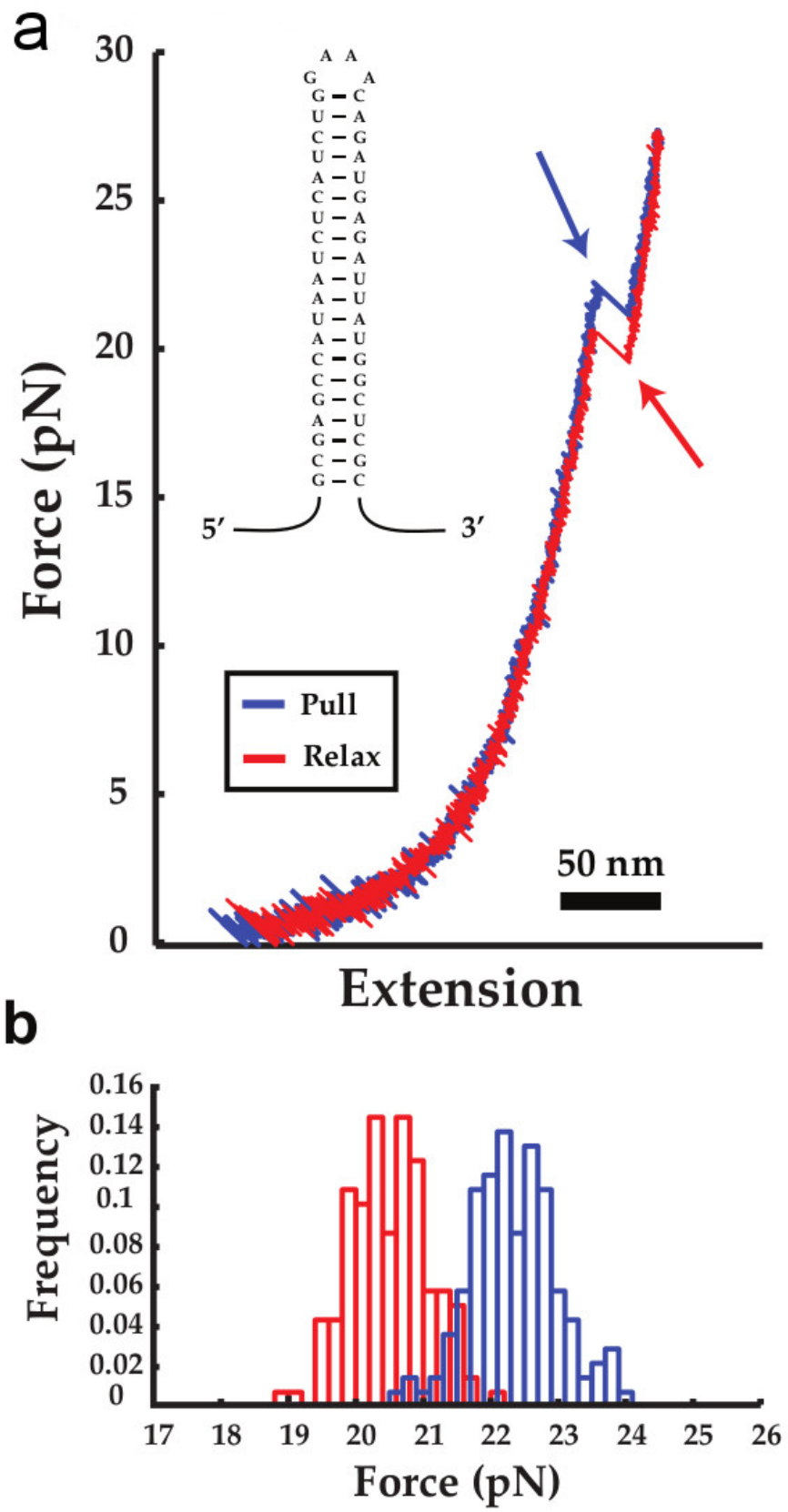

Figure 8. Force ramp. a) A force-extension curve of mechanically unfolding of a hairpin. Pulling is shown in blue and relaxation in red. The unfolding/refolding of the hairpin are indicated by the arrows. **b)** Distributions of unfolding (blue) and refolding (red) forces of the hairpin. The figure is adapted from a submitted manuscript[39].

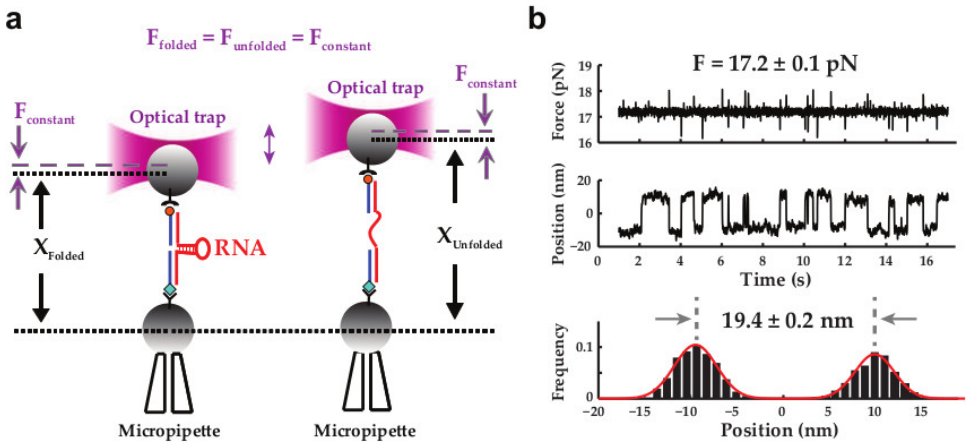

Figure 9. An RNA hairpin under constant force. a) Diagram of experiment. The position of the trap is changed through feedback so as to maintain a constant force on the hairpin. **b)** Force and position versus time for hairpin un/folding. As the force is kept constant, the position of the trap fluctuates between two values, showing bistability of the hairpin at the force. The binomial distribution of the trap distribution yields the extension change upon the hairpin unfolding of 19.4 ±0.2 nm. The figure is adapted from a submitted manuscript[39].

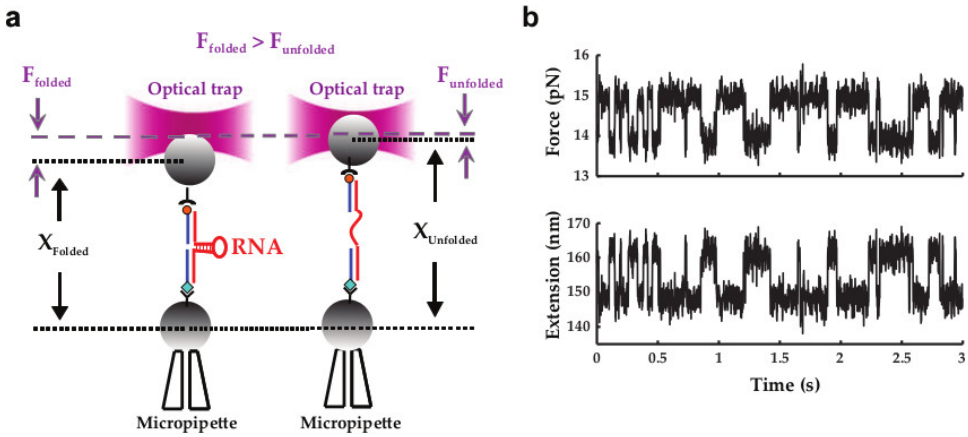

Figure 10. Passive mode of a hairpin. a) Diagram of experiment. The positions of the trap and the micropipette are fixed. When the molecule unfolds, the extension increases and the trapped bead moves towards the center of the trap, reducing the force. When the RNA folds, the extension shortens, which brings the trapped bead away from the center of the trap, increasing the force. **b)** Force and extension versus time of a hairpin under passive mode.

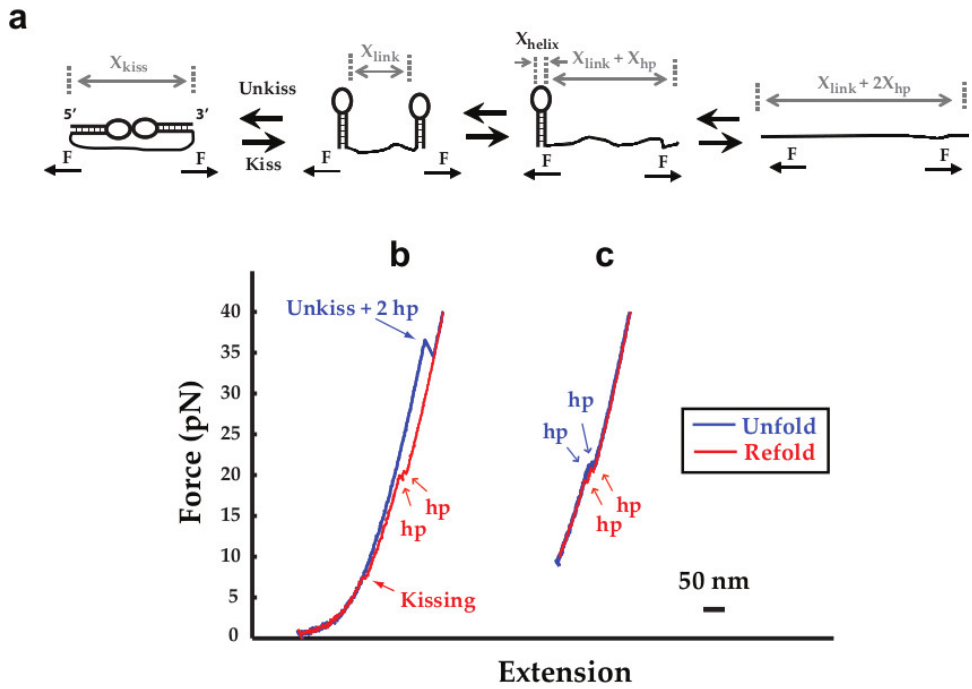

Figure 11. Force ramp of the two-base-pair kissing RNA. a) Hierarchical folding of a two-base-pair kissing RNA under mechanical tension. **b)** Force-extension curve. Structural transitions are indicated by arrows. **c)** Force-extension curve when the lowest force is set at 10 pN to prevent the kissing interaction. The figure is adapted with permission from Journal of American Chemical Society[34].

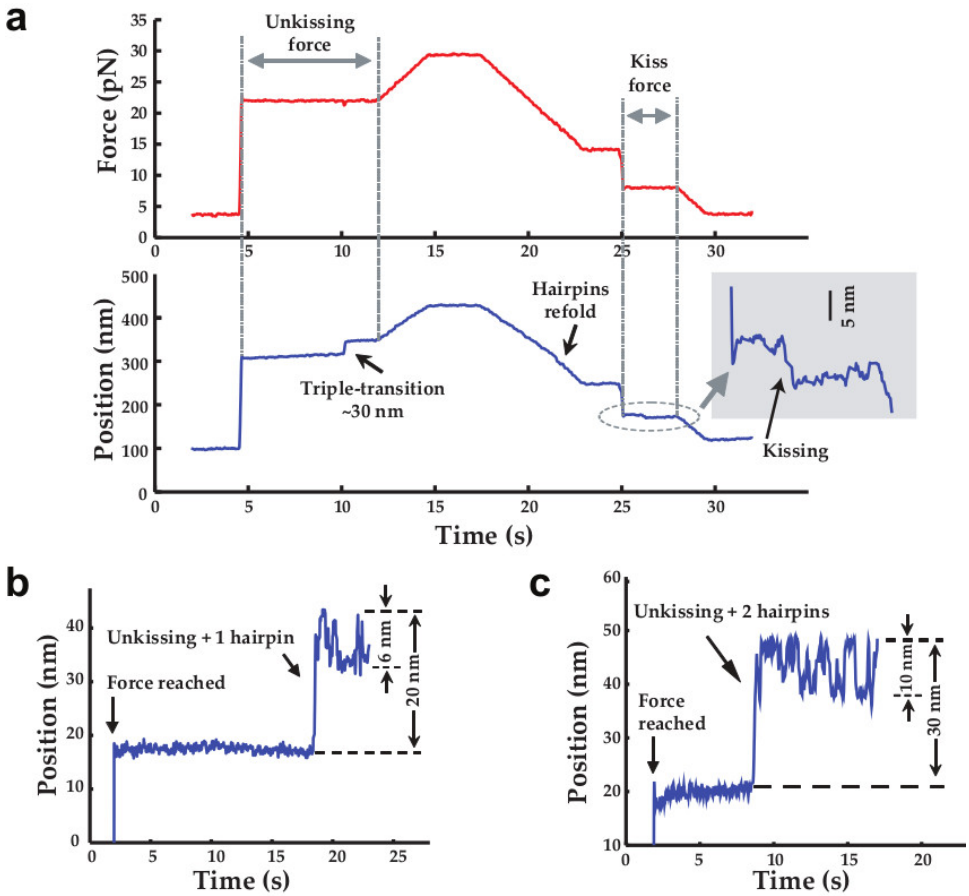

Figure 12. Force jump of the two-base-pair kissing RNA. a) A force jump/drop cycle to measure unkissing and kissing lifetimes at two different forces. The top panel shows the time trace of force. The bottom panel shows the relative extension of the molecule. The force is first jumped from 3 pN to 22 pN to measure the lifetime of the kissing complex at 22 pN. The unkissing is indicated by a quick increase in extension by ~30 nm, indicating the entire RNA is unfolded into a single strand. On relaxation, force is ramped down to 14 pN to allow the two hairpins to refold. The force is then dropped to 8 pN. Formation of the kissing interaction is indicated by decrease in extension of ~ 7-8 nm. **b)** As force is jumped to 16 pN, the time-extension trace shows that it takes several seconds for the kissing complex and the seven-base-pair hairpin to unfold, after which the hairpin unfolds and refolds rapidly. **c)** The entire kissing complex is unfolded into a single strand a few seconds after force is jumped to 17.7 pN. The remaining trace shows the bistability of the 11-base-pair hairpin. Each of the structural transitions in unfolding the kissing RNA shows distinctive X. The figure is adapted with permission from Proceedings of National Academy of Sciences [28].

Reagent	*µL*
Plasmid (10 ng/mL)	10
Primer T7f (100 mM)	10
Primer Br (100 mM)	10
dNTP mix (25 mM each)	10
10x PCR buffer	100
H_2O	850
Taq DNA polymerase	10
Total	**1,000**

Note: A typical thermal cycle for synthesizing 3 kbp DNA is: 95 °C 45 seconds, 53 °C 1 minute, 72 °C 3 minutes.

Table 1. An example of PCR for synthesizing transcription template.

Reagent	*µL*
template (>200 ng/mL)	8
NTPs	8 (2 mL each)
10x reaction buffer	2

T7 RNA polymerase	2
Total	20

Note: Incubate the reaction at 37 °C overnight.

Table 2. In vitro transcription.

Reagent	*μL*
Handle A (~10 mg)	50
Biotin-11UTP	5
T4 pol reaction buffer	5
BSA solution	1
T4 DNA polymerase	5
Total	66

Note: Incubate the reaction at room temperature for 20 minutes. Inactivate the enzyme by heating at 70 °C for 20 minutes, followed by slow cooling to room temperature.

Table 3. Primer extension reaction.

Reagent	*μL*
Formamide	800
EDTA (0.5 M, pH 8.0)	2
PIPES (1 M, pH 6.3)	40
NaCl (5M)	80
Total	922

Table 4. Recipe of the anneal buffer.

Reagent	
Biotin-HA	1,000 ng
Dig-HB	1,000 ng
RNA	1,000 ng
Annealing buffer	80 mL

Note: A typical thermal cycle for annealing is: 95 °C 10 minutes, 62 °C 1 hour, 52 °C 1 hour, followed by ramping to 4 °C.

Table 5. Anneal RNA with handles.

Discussion

Modification and Troubleshooting in Preparation of Tweezing Samples

Choice of Cloning Vector. Although the general scheme described here (**Figure 3**) does not require a special cloning vector, the vector is preferred not to have intrinsic T7 or T3 promoter for the ease of transcription such that a promoter can be introduced via PCR at desired positions.

Sequence and Lengths of the Handles. There is no specific sequence requirement for the handles. However, a close GC to AT ratio is preferred, whereas homopolymeric and highly repeated sequences should be avoided. In published works, the two handles are kept as similar lengths such that the RNA structure of interest is placed roughly in the middle. Previous work shows that the total length of the handles varied from 500 to 10,000 base pairs subtly affects the measured kinetics[46,47].

Quality Check and Quantitation of the Annealed Mixture. Besides the intended RNA with handles, the final product also contains unannealed DNA handles and RNAs, as well as others. It is difficult and uneconomical to purify the tweezing molecules. Instead, the annealed mixture can be directly used for tweezing, because only the properly annealed nucleic acids can be tethered to two surface-coated beads. Properly annealed product is also difficult to be distinguished from the handles and the RNA on agarose gel electrophoresis. The best way to test the quality and to quantify the concentration of the annealed product is to test it on the tweezers. However, it is helpful to check and quantify the PCR and transcription products in each step using various molecular biology techniques.

Alternative Approaches to Tether RNA to Beads. There are many conceivable methods to link RNA molecules to surfaces covalently or non-covalently[48]. The approach described in this work is one of the simplest and most robust methods employed in several RNA tweezing labs.

Single- vs. Multiple-molecule Tether. A pair of strep- and dig-beads can be linked by multiple molecules. To tease out such a possibility of multiple molecules tethering the bead, the force-distance curves need to be closely examined. Single-molecule tether display a worm-like-chain elasticity[4] that is generally unseen in multi-molecule tethers. Additional control experiments specific for each system may be required for confirming the single-molecule tether.

Improvements of the Minitweezers

Fast and Slow Data Recording. The Minitweezers has a built-in data acquisition that records up to 21 instrumental parameters at a rate of 200 Hz in a computer, which will be referred as the operating computer in this work. However, some applications and calibrations require a fast data acquisition rate. To this end, the electronic signals of force and distance are split to be recorded in a new computer, the “fast-recording” computer, in addition to the data acquisition in the operating computer. The fast-recording computer reads data through a separate data acquisition card and software, which allows multiple channels at up to 1 MHz. The new computer and data acquisition does not interfere with the operation of the instrument, which is solely controlled by the operating computer. In an experiment, data are simultaneously recorded on both computers at different rates. Time synchronization is performed during data analysis by comparing the corresponding data files.

Video Image Recording. A video card and imaging software are installed on the fast-recording computer to capture live images of the reaction and to analyze video images. This development makes it possible to implement the pixel size and distance calibrations described above.

Limitations and Future Applications of the Method

Methods to precisely manipulate and measure conformational changes of a single RNA molecule have been discussed. Such abilities make it possible to monitor structural rearrangement of an RNA strand in real time. Furthermore, force can be used to influence the RNA structure and folding pathways, allowing rare and/or less than optimal structures to be folded.

However, there are limitations of the mechanical approach. Most importantly, the extension, which is used to interpret conformational changes, is a one-dimensional projection of the three-dimensional structures. It is possible that some conformational changes cannot be measured[49-52], and/or kinetic barriers are hidden from observation[53]. There are also various instrumental effects and limitations that may affect the observed thermodynamics and kinetics[44,46,47].

The optical tweezers have been applied to study a limited number of RNA structures, as compared to numerous transcripts suggested by genome-wide surveys[54]. The technique will be used to study different structural motifs and large RNAs. In addition, the method will find new applications in RNA research. For example, RNA-binding ligand and proteins may stabilize or change the RNA structure, which can be measured using the mechanical approach.

Disclosures

The authors have nothing to disclose.

Acknowledgements

This work was supported by an NSF grant (MCB-1054449) and a collaborative interdisciplinary Pilot Research Program award from The RNA Institute at University at Albany to PTXL.

References

1. Ashkin, A. Optical trapping and manipulation of neutral particles using lasers. *Proceedings of the National Academy of Sciences of the United States of America.* **94**, 4853-4860 (1997).
2. Maier, B. Using laser tweezers to measure twitching motility in Neisseria. *Current opinion in microbiology.* **8**, 344-349, doi:10.1016/j.mib.2005.04.002 (2005).
3. Wang, S., Arellano-Santoyo, H., Combs, P. A., & Shaevitz, J. W. Measuring the bending stiffness of bacterial cells using an optical trap. *Journal of visualized experiments : JoVE.*(38), doi:10.3791/2012 (2010).
4. Smith, S. B., Cui, Y., & Bustamante, C. Overstretching B-DNA: the elastic response of individual double-stranded and single-stranded DNA molecules. *Science (New York, N.Y.).* **271**, 795-799 (1996).
5. Strick, T. R., Allemand, J. F., Bensimon, D., Bensimon, A., & Croquette, V. The elasticity of a single supercoiled DNA molecule. *Science (New York, N.Y.).* **271**, 1835-1837 (1996).
6. Bryant, Z. *et al.* Structural transitions and elasticity from torque measurements on DNA. *Nature.* **424**, 338-341, doi:10.1038/nature01810 (2003).
7. Liphardt, J., Onoa, B., Smith, S. B., Tinoco, I., J., & Bustamante, C. Reversible unfolding of single RNA molecules by mechanical force. *Science (New York, N.Y.).* **292**, 733-737 (2001).
8. Li, P. T. X., Vieregg, J., & Tinoco, I., Jr. How RNA unfolds and refolds. *Annu Rev Biochem.* **77**, 27.21-24 (2008).
9. Woodside, M. T., Garcia-Garcia, C., & Block, S. M. Folding and unfolding single RNA molecules under tension. *Current opinion in chemical biology.* **12**, 640-646, doi:10.1016/j.cbpa.2008.08.011 (2008).
10. Cecconi, C., Shank, E. A., Bustamante, C., & Marqusee, S. Direct observation of the three-state folding of a single protein molecule. *Science (New York, N.Y.).* **309**, 2057-2060, doi:10.1126/science.1116702 (2005).
11. Shank, E. A., Cecconi, C., Dill, J. W., Marqusee, S., & Bustamante, C. The folding cooperativity of a protein is controlled by its chain topology. *Nature.* **465**, 637-640, doi:10.1038/nature09021 (2010).
12. Morin, J. A. *et al.* Active DNA unwinding dynamics during processive DNA replication. *Proceedings of the National Academy of Sciences of the United States of America.* **109**, 8115-8120, doi:10.1073/pnas.1204759109 (2012).

Copyright © 2014 Journal of Visualized Experiments

13. Larson, M. H., Landick, R., & Block, S. M. Single-molecule studies of RNA polymerase: one singular sensation, every little step it takes. *Molecular cell.* **41**, 249-262, doi:10.1016/j.molcel.2011.01.008 (2011).
14. Wen, J. D. *et al.* Following translation by single ribosomes one codon at a time. *Nature.* **452**, 598-603, doi:10.1038/nature06716 (2008).
15. Qu, X. *et al.* The ribosome uses two active mechanisms to unwind messenger RNA during translation. *Nature.* **475**, 118-121, doi:10.1038/nature10126 (2011).
16. Pease, P. J. *et al.* Sequence-directed DNA translocation by purified FtsK. *Science (New York, N.Y.).* **307**, 586-590, doi:10.1126/science.1104885 (2005).
17. Dumont, S. *et al.* RNA translocation and unwinding mechanism of HCV NS3 helicase and its coordination by ATP. *Nature.* **439**, 105-108, doi:10.1038/nature04331 (2006).
18. Greenleaf, W. J., Woodside, M. T., & Block, S. M. High-resolution, single-molecule measurements of biomolecular motion. *Annual review of biophysics and biomolecular structure.* **36**, 171-190, doi:10.1146/annurev.biophys.36.101106.101451 (2007).
19. Serganov, A., & Nudler, E. A decade of riboswitches. *Cell.* **152**, 17-24, doi:10.1016/j.cell.2012.12.024 (2013).
20. Breaker, R. R. Prospects for riboswitch discovery and analysis. *Molecular cell.* **43**, 867-879, doi:10.1016/j.molcel.2011.08.024 (2011).
21. Wan, Y. *et al.* Genome-wide measurement of RNA folding energies. *Molecular cell.* **48**, 169-181, doi:10.1016/j.molcel.2012.08.008 (2012).
22. Dalgarno, P. A. *et al.* Single-molecule chemical denaturation of riboswitches. *Nucleic acids research.* **41**, 4253-4265, doi:10.1093/nar/gkt128 (2013).
23. Wood, S., Ferre-D'Amare, A. R., & Rueda, D. Allosteric tertiary interactions preorganize the c-di-GMP riboswitch and accelerate ligand binding. *ACS chemical biology.* **7**, 920-927, doi:10.1021/cb300014u (2012).
24. Brenner, M. D., Scanlan, M. S., Nahas, M. K., Ha, T., & Silverman, S. K. Multivector fluorescence analysis of the xpt guanine riboswitch aptamer domain and the conformational role of guanine. *Biochemistry.* **49**, 1596-1605, doi:10.1021/bi9019912 (2010).
25. Greenleaf, W. J., Frieda, K. L., Foster, D. A., Woodside, M. T., & Block, S. M. Direct observation of hierarchical folding in single riboswitch aptamers. *Science (New York, N.Y.).* **319**, 630-633, doi:10.1126/science.1151298 (2008).
26. Frieda, K. L., & Block, S. M. Direct observation of cotranscriptional folding in an adenine riboswitch. *Science (New York, N.Y.).* **338**, 397-400, doi:10.1126/science.1225722 (2012).
27. Neupane, K., Yu, H., Foster, D. A., Wang, F., & Woodside, M. T. Single-molecule force spectroscopy of the add adenine riboswitch relates folding to regulatory mechanism. *Nucleic acids research.* **39**, 7677-7687, doi:10.1093/nar/gkr305 (2011).
28. Li, P. T. X., Bustamante, C., & Tinoco, I., Jr. Unusual Mechanical Stability of A Minimal RNA Kissing Complex. *Proc. Natl. Acad. Sci. U. S. A.* **103**, 15847-15852 (2006).
29. Li, P. T. X., Bustamante, C., & Tinoco, I., Jr. Real-time control of the energy landscape by force directs the folding of RNA molecules. *Proc. Natl. Acad. Sci. U. S. A.* **104**, 7039-7044 (2007).
30. Tinoco, I., Jr, Li, P. T. X., & Bustamante, C. Determination of ther modynamics and kinetics of RNA reactions by force. *Q. Rev. Biophys.* **39**, 325-360 (2006).
31. Onoa, B. *et al.* Identifying kinetic barriers to mechanical unfolding of the T. thermophila ribozyme. *Science (New York, N.Y.).* **299**, 1892-1895 (2003).
32. Li, P. T., & Tinoco, I., Jr. Mechanical unfolding of two DIS RNA kissing complexes from HIV-1. *J Mol Biol.* **386**, 1343-1356 (2009).
33. Smith, S., Cui, Y., & Bustamante, C. Optical-trap force transducer that operates by direct measurement of light momentum. *Methods Enzymol.* **361**, 134-162 (2003).
34. Stephenson, W. *et al.* The essential role of stacking adenines in a two-base-pair RNA kissing complex. *J Am Chem Soc.* **135**, 5602-5611 (2013).
35. Kaiser, C. M., Goldman, D. H., Chodera, J. D., Tinoco, I., Jr., & Bustamante, C. The ribosome modulates nascent protein folding. *Science (New York, N.Y.).* **334**, 1723-1727, doi:10.1126/science.1209740 (2011).
36. Bizarro, C. V., Alemany, A., & Ritort, F. Non-specific binding of Na+ and Mg2+ to RNA determined by force spectroscopy methods. *Nucleic acids research.* **40**, 6922-6935, doi:10.1093/nar/gks289 (2012).
37. Bosaeus, N. *et al.* Tension induces a base-paired overstretched DNA conformation. *Proceedings of the National Academy of Sciences of the United States of America.* **109**, 15179-15184, doi:10.1073/pnas.1213172109 (2012).
38. Berg-Sørensen, K., & Flyvbjerg, H. Power spectrum analysis for optical tweezers. *Rev. Sci. Instrum. .* **75**, 594-612 (2004).
39. Stephenson, W. *et al.* Combining temperature and force to study folding of an RNA hairpin. *Phys. Chem. Chem. Phys. .* **16**, 906-917 (2014).
40. Evans, E., & Ritchie, K. Dynamic strength of molecular adhesion bonds. *Biophys. J.* **72**, 1541-1555 (1997).
41. Dudko, O. K., Hummer, G., & Szabo, A. Intrinsic rates and activation free energies from single-molecule pulling experiments. *Phys. Rev. Lett.* **96**, 108101 (2006).
42. Dudko, O. K., Hummer, G., & Szabo, A. Theory, analysis, and interpretation of single-molecule force spectroscopy experiments. *Proc. Natl. Acad. Sci. U. S. A.* **105**, 15755-15760 (2008).
43. Li, P. T. X., Collin, D., Smith, S. B., Bustamante, C., & Tinoco, I., Jr. Probing the Mechanical Folding Kinetics of TAR RNA by Hopping, Force-Jump and Force-Ramp Methods. *Biophys. J.* **90**, 250-260 (2006).
44. Elms, P. J., Chodera, J. D., Bustamante, C. J., & Marqusee, S. Limitations of constant-force-feedback experiments. *Biophysical journal.* **103**, 1490-1499, doi:10.1016/j.bpj.2012.06.051 (2012).
45. Li, P. T. X. Analysis of Diffuse K+ and Mg2+ Ion Binding to a Two-Base-Pair Kissing Complex by Single-Molecule Mechanical Unfolding. *Biochemistry.* **52**, 4991-5001 (2013).
46. Wen, J. D. *et al.* Force unfolding kinetics of RNA using optical tweezers. I. Effects of experimental variables on measured results. *Biophys. J.* **92**, 2996-3009 (2007).
47. Manosas, M. *et al.* Force Unfolding Kinetics of RNA using Optical Tweezers. II. Modeling Experiments. *Biophys. J.* **92**, 3010-3021 (2007).
48. Vilfan, I. D. *et al.* An RNA toolbox for single-molecule force spectroscopy studies. *Nucleic acids research.* **35**, 6625-6639, doi:10.1093/nar/gkm585 (2007).
49. Li, P. T. X. Formation of a metastable intramolecular RNA kissing complex by nanomanipulation. *Soft Matter.* **9**, 3246-3254 (2013).
50. Chen, G., Chang, K. Y., Chou, M. Y., Bustamante, C., & Tinoco, I., Jr. Triplex structures in an RNA pseudoknot enhance mechanical stability and increase efficiency of -1 ribosomal frameshifting. *Proceedings of the National Academy of Sciences of the United States of America.* **106**, 12706-12711, doi:10.1073/pnas.0905046106 (2009).
51. Chen, G., Wen, J. D., & Tinoco, I., Jr. Single-molecule mechanical unfolding and folding of a pseudoknot in human telomerase RNA. *RNA (New York, N.Y.).* **13**, 2175-2188, doi:10.1261/rna.676707 (2007).

Copyright © 2014 Journal of Visualized Experiments

52. Tinoco, I., Chen, G., & Qu, X. RNA reactions one molecule at a time. *Cold Spring Harbor perspectives in biology.* **2**, a003624, doi:10.1101/cshperspect.a003624 (2010).
53. Dudko, O. K., Graham, T. G., & Best, R. B. Locating the barrier for folding of single molecules under an external force. *Physical review letters.* **107**, 208301 (2011).
54. Djebali, S. *et al.* Landscape of transcription in human cells. *Nature.* **489**, 101-108, doi:10.1038/nature11233 (2012).

Copyright © 2014 Journal of Visualized Experiments